

Proton radioactivity with a Yukawa effective interaction

T. R. Routray¹, S. K. Tripathy¹, B. B. Dash¹, B. Behera¹ and D.N. Basu^{2 a}

¹ P.G. Department of Physics, Sambalpur University, Jyoti Vihar, Burla, Orissa 768019, India

² Variable Energy Cyclotron Centre, 1/AF Bidhan Nagar, Kolkata 700 064, India.

April 27, 2011

Abstract. The half lives of proton radioactivity of proton emitters are investigated theoretically. Proton-nucleus interaction potentials are obtained by folding the densities of the daughter nuclei with a finite range effective nucleon-nucleon interaction having Yukawa form. The Wood-Saxon density distributions for the nuclei used in calculating the nuclear as well as the Coulomb interaction potentials are predictions of the interaction. The quantum mechanical tunneling probability is calculated within the WKB framework. These calculations provide reasonable estimates for the observed proton radioactivity lifetimes. The effects of neutron-proton effective mass splitting in neutron rich asymmetric matter as well as the nuclear matter incompressibility on the decay probability are investigated.

Keywords: Proton Radioactivity; Folding model; WKB; Finite range Yukawa interaction.

PACS. 23.50.+z, 21.30.Fe, 25.55.Ci, 21.65.+f

1 Introduction

In recent years new half life measurements have been performed in order to have a better understanding of the proton and alpha decay processes in the region of proton-rich nuclei [1]. For these nuclei the Q value for proton emissions is positive and therefore there is a natural tendency to shed off excess protons. These data are very useful for the analysis of possible irregularities in the structure of these proton-rich nuclei [2,3]. They are also of great interest in rapid proton capture nucleosynthesis processes. Some new results for proton radioactivity in this region of proton-rich nuclei have indicated that the proton emission mode is rather competitive with the alpha decay process [3,4,5]. Proton radioactivity may be used as a tool to obtain spectroscopic information because the decaying proton is unpaired in the orbit. These decay rates are sensitive to the Q values and the orbital angular momenta which in turn help to determine the orbital angular momenta of the emitted protons.

Since the observation of proton radioactivity is comparatively recent, several theoretical approaches that have been employed to study this exotic process, such as the distorted-wave Born approximation [6], the density dependent M3Y (DDM3Y) effective interaction [7,8], the effective interaction of Jeukenne, Lejeune and Mahaux (JLM) [8], the unified fission model [9], the coupled-channels approach [10] and the effective/generalized liquid drop models [11,12] are also quite recent [13,14]. In the present

work, quantum mechanical tunneling probability is calculated within the WKB framework using proton-nucleus interaction potentials obtained from folding the density of the residual daughter nucleus with a finite range effective nucleon-nucleon interaction having a single Yukawa term (YENI) in the finite range part [15,16]. These calculations provide good estimates for the observed proton radioactivity lifetimes. In the present calculation we shall examine the effects of neutron-proton (n-p) effective mass splitting as well as the nuclear matter incompressibility, $K(\rho_0)$, on the decay probability of the proton emitters. The n-p effective mass splitting is connected to the momentum dependence aspect of neutron and proton mean fields in asymmetric nuclear matter (ANM). Theoretical predictions of different models on this important issue can be divided into two distinct groups depending on whether the neutron effective mass goes above the proton one [17,18,19,20,21,22] or the other way around [23,24,25,26,27]. Experimental as well as theoretical attempts [28,29] to resolve the problem has not been successful as yet. In the work in Ref.[16] it is shown that if the finite range exchange interaction acting between an unlike nucleon pair, $v_{ex}^{ul}(r)$, is stronger compared to the finite range exchange interaction, v_{ex}^l , between a pair of like nucleon, the neutron effective mass will be predicted to go over the proton one in neutron rich ANM. On the other hand if $v_{ex}^l(r)$ is stronger compared to $v_{ex}^{ul}(r)$ then proton effective mass will go over the neutron one. The results of Dirac-Brueckner-Hartree-Fock (DBHF) calculations [19,21] along with the decreasing trend of Lane potential extracted from experimental data on nucleon-nucleus scattering and reaction [30,31,

^a trr1@rediffmail.com;
dnb@veccal.ernet.in

bibhutiphy@rediffmail.com;

32,33] has led to accept amongst a larger community that neutron effective mass goes above the proton one in neutron rich matter although the controversy is not yet completely resolved. Under the circumstance the magnitude of effective mass splitting remains as an open problem as different models give widely divergent results. Similarly, the nuclear matter incompressibility is another important quantity whose value ranges between 240 ± 20 MeV as has been estimated from studies of isoscalar giant monopole resonances in nuclei. In the present work we shall also examine the possible effect of the variations of these nuclear matter parameters on the calculated proton half-lives of the proton emitters.

In section 2 the calculation of proton-nucleus (p-N) interaction potential for any general effective interaction has been discussed. The formalism has been extended to the calculation with the YENI. The determination of the parameters required in the study of the nuclear matter is briefly discussed. The fixation of the free parameter of the interaction along with the Wood-Saxon (WS) density distribution for the nuclei have been obtained by adopting a simultaneous minimization procedure to reproduce the binding energies of nuclei. Contributions of the different parts of YENI to the p-N nuclear potential and the self-consistent evaluation of the finite range exchange part are provided. In section 3 WKB tunneling procedure for calculation of decay probability of emitted proton has been discussed. The last section contains discussions of the results obtained and conclusions.

2 The proton-nucleus interaction potentials

2.1 The folded proton-nucleus interaction potential

The proton-nucleus potential is obtained by folding the density distribution of the nucleus over the interaction of the incident proton with nucleons of the nucleus. It is given by [34]

$$V_N(\mathbf{r}) = \int [\rho_p(\mathbf{r}') v_d^{pp}(|\mathbf{r} - \mathbf{r}'|) + \rho_n(\mathbf{r}') v_d^{pn}(|\mathbf{r} - \mathbf{r}'|)] d^3 r' \\ + \int \rho_p(\mathbf{r}, \mathbf{r}') j_0(k(\mathbf{R})|\mathbf{r} - \mathbf{r}'|) v_{ex}^{pp}(|\mathbf{r} - \mathbf{r}'|) d^3 r' \\ + \int \rho_n(\mathbf{r}, \mathbf{r}') j_0(k(\mathbf{R})|\mathbf{r} - \mathbf{r}'|) v_{ex}^{pn}(|\mathbf{r} - \mathbf{r}'|) d^3 r' \\ + \text{rearrangement terms} \quad (1)$$

where \mathbf{r} and \mathbf{r}' are the distances of the incident proton and the nucleon of the nucleus, respectively, from the origin taken at the center of the nucleus. The last term in Eq.(1) is the rearrangement term that arises from the explicit density dependence of the effective interaction. $\rho_i(\mathbf{r}, \mathbf{r}')$, $i = p, n$ are the density matrices that take non-local effects into account, and $v_{d/ex}$ is the direct/exchange part of the effective interaction averaged over space, spin and isospin of both the interacting nucleons. j_0 is the zeroth order spherical Bessel function. $k(\mathbf{R})$ is the wave number of the incident proton at the center of mass \mathbf{R} of the incident proton and nucleon of the nucleus and is given by,

$$k(\mathbf{R}) = \sqrt{\frac{2\mu}{\hbar^2} (E_{cm} - V_N(\mathbf{R}) - V_c(\mathbf{R}))} \quad (2)$$

where E_{cm} , $V_N(\mathbf{R})$ and $V_c(\mathbf{R})$ are the center of mass energy, p-N interaction potential and Coulomb potential at the center of mass \mathbf{R} , respectively. The center of mass and relative coordinates are given by $\mathbf{R} = (\mathbf{r} + \mathbf{r}')/2$ and $\mathbf{t} = (\mathbf{r} - \mathbf{r}')$ respectively. It may be seen from Eq.(1) that in the calculation of $V_N(\mathbf{r})$ the knowledge of $k(\mathbf{R})$ is required in which $V_N(\mathbf{R})$ appears and hence requires a self-consistent calculation. The total interaction energy between the proton and the residual daughter nucleus $V(\mathbf{r}) = V_N(\mathbf{r}) + V_C(\mathbf{r}) + \hbar^2 l(l+1)/(2\mu r^2)$, the sum of the nuclear interaction energy, the Coulomb interaction energy and the centrifugal barrier where l is the angular momentum carried away by the proton-daughter nucleus system. Here $\mu = M_p M_d / M_A$ is the reduced mass, M_p , M_d and M_A are the masses of the proton, the daughter nucleus and the parent nucleus respectively, all measured in the units of MeV/ c^2 .

2.2 Simple finite range effective interaction and the proton-nucleus potential

The simple parameterization of finite range effective interaction [16] used in this work for calculating proton radioactivity of the spontaneous proton emitters is given by,

$$v_{eff}(\mathbf{r} - \mathbf{r}') = t_0(1 + x_0 P_\sigma) \delta(\mathbf{r} - \mathbf{r}') \\ + \frac{t_3}{6} (1 + x_3 P_\sigma) \left[\frac{\rho(\mathbf{R})}{1 + b\rho(\mathbf{R})} \right]^\gamma \delta(\mathbf{r} - \mathbf{r}') \\ + (W + B P_\sigma - H P_\tau - M P_\sigma P_\tau) f_\alpha(|\mathbf{r} - \mathbf{r}'|) \quad (3)$$

where $f_\alpha(|\mathbf{r} - \mathbf{r}'|)$, is a short range interaction of conventional form, such as, Yukawa, Gaussian or exponential and specified by a single parameter α , the range of interaction. This effective interaction contains altogether eleven adjustable parameters, namely, $t_0, x_0, t_3, x_3, b, \gamma, W, B, H, M$ and α . $P_\sigma = (1 + \boldsymbol{\sigma}_1 \cdot \boldsymbol{\sigma}_2)/2$ and $P_\tau = (1 + \boldsymbol{\tau}_1 \cdot \boldsymbol{\tau}_2)/2$ are the spin and isospin exchange operators respectively. This interaction has been used in the studies of momentum and density dependence of both symmetric and asymmetric nuclear matter at zero and finite temperatures [15,16] as well as in the calculation of bulk properties of neutron stars [35] and equation of state (EOS) of beta stable $n+p+e+\mu$ matter, i.e., neutron star matter (NSM) [36]. In these studies we require a total of nine parameter combinations, namely, $\alpha, b, \gamma, \varepsilon_0^l, \varepsilon_0^{ul}, \varepsilon_\gamma^l, \varepsilon_\gamma^{ul}, \varepsilon_{ex}^l$ and ε_{ex}^{ul} out of the total eleven interaction parameters for the complete description of asymmetric nuclear matter and their relations to the interaction parameters are given in Ref. [35]. Out of these nine parameters required for a complete description of ANM only six, namely $\alpha, b, \gamma, (\varepsilon_0^l + \varepsilon_0^{ul}), (\varepsilon_\gamma^l + \varepsilon_\gamma^{ul})$ and $(\varepsilon_{ex}^l + \varepsilon_{ex}^{ul})$ are required to describe the EOS of symmetric nuclear matter (SNM). The careful adjustment of these six parameters so as to provide a correct momentum

dependence of the mean field as well as density dependence of the EOS in SNM is discussed in the Refs.[35,37]. The crucial advantage of the procedure adopted to constrain these six parameters in SNM is that the momentum dependence of the mean field can be varied without changing the density dependence of the EOS of SNM and vice-versa is also true. The momentum dependence of the mean field in SNM is decided by the finite range exchange strength parameter $(\varepsilon_{ex}^l + \varepsilon_{ex}^{ul})$ and the range α , whereas, the stiffness of the EOS is determined by the parameter γ in the exponent. Under the consideration that the interaction between pairs of like (l) and unlike (ul) nucleons have same range but differ in strength, the study of ANM now, requires the correct splittings of the three parameters $(\varepsilon_0^l + \varepsilon_0^{ul})$, $(\varepsilon_\gamma^l + \varepsilon_\gamma^{ul})$ and $(\varepsilon_{ex}^l + \varepsilon_{ex}^{ul})$ into two specific channels for interaction between pairs of like and unlike nucleons. In absence of adequate constraints, either experimental or theoretical, to decide the splitting of these three strength parameters the procedure that we have adopted in our study of ANM has been discussed in Refs.[16,35]. The splitting of finite range exchange strength parameter $(\varepsilon_{ex}^l + \varepsilon_{ex}^{ul})$ into like and unlike channels decides the n - p effective mass splitting in ANM. The possible range of splitting into the like channel, i.e., ε_{ex}^l , can be from 0 to $(\varepsilon_{ex}^l + \varepsilon_{ex}^{ul})$ and accordingly the exchange strength in the unlike channel ε_{ex}^{ul} is decided. For ε_{ex}^l in between 0 and $(\varepsilon_{ex}^l + \varepsilon_{ex}^{ul})/2$ the neutron effective mass is predicted to lie over the proton one and for ε_{ex}^l in the range $(\varepsilon_{ex}^l + \varepsilon_{ex}^{ul})/2$ and $(\varepsilon_{ex}^l + \varepsilon_{ex}^{ul})$ the vice-versa is the case. For a given ε_{ex}^l the splitting of one of the rest two strength parameters, $(\varepsilon_0^l + \varepsilon_0^{ul})$ and $(\varepsilon_\gamma^l + \varepsilon_\gamma^{ul})$, can be decided by assuming a standard value of symmetry energy $E_s(\rho_0)$ at normal density ρ_0 . The splitting of the remaining parameter is decided from the value of $E'_s(\rho_0) = \rho_0 \frac{dE_s(\rho)}{d\rho}|_{\rho=\rho_0}$. In order to decide the value of $E'_s(\rho_0)$ we have assigned arbitrary values to it and calculated the EOS of NSM in each case solving the charge neutrality and beta stability conditions. It is found that for a characteristic value of $E'_s(\rho_0)$ the asymmetric contribution to the nucleonic part of the EOS of NSM (that solely determines the composition of normal neutron stars) gives stiffest behaviour that remains almost stationary within a small range around this value of $E'_s(\rho_0)$ [35]. This is referred as the universal high density behaviour of the asymmetric contribution of the nucleonic part of the EOS in NSM. We have considered this characteristic value of $E'_s(\rho_0)$ that corresponds to the stiffest behaviour. For the standard value of $E_s(\rho_0) = 30$ MeV, the value of $E'_s(\rho_0)$ is obtained to be 21.51 MeV for the EOS having $\gamma = 1/2$ and $\varepsilon_{ex}^l = (\varepsilon_{ex}^l + \varepsilon_{ex}^{ul})/3$. $E'_s(\rho_0)$ varies from 20.93 MeV to 22.08 MeV as ε_{ex}^l changes from 0 to $(\varepsilon_{ex}^l + \varepsilon_{ex}^{ul})/2$ showing a small variation. Similarly $E'_s(\rho_0)$ also shows a slow variation on the choice of γ where it varies from 20.98 MeV to 21.70 MeV as γ varies from 1/3 to 2/3 (corresponding to nuclear matter incompressibility in the range 220 to 253 MeV) for $\varepsilon_{ex}^l = (\varepsilon_{ex}^l + \varepsilon_{ex}^{ul})/3$. The slope parameter $L = 3E'_s(\rho_0)$ thus predicted for the EOSs considered lie within the range obtained from simultaneous analysis of neutron skin thickness results in nuclei and neutron star properties [38,39,40]. Now, with

the knowledge of all these nine parameters we are still left with two interaction parameters free for the calculation of finite nucleus. Here we considered t_0 and x_0 of our interaction in Eq.(3) as the free parameters. We determine the parameter t_0 by using a simultaneous minimization along with the WS density distribution parameters to fit to the binding energy of ^{40}Ca nucleus.

2.3 Determination of the parameter t_0 and Wood-Saxon density distribution of nucleus

The total energy of a nucleus is given by $E = E^{nucl} + E^{Coul} + E^{CM}$, where E^{nucl} , E^{Coul} and E^{CM} are the contributions from nuclear, Coulomb and center-of-mass correction, respectively. The nuclear part of the energy for an effective interaction is given by,

$$E^{nucl} = \frac{\hbar^2}{2M} \int [\tau_n(\mathbf{r}) + \tau_p(\mathbf{r})] d^3r + \sum_{s,s'=n,p} \left[\frac{1}{2} \int \int \rho_s(\mathbf{r}) \rho_{s'}(\mathbf{r}') v_d^{ss'}(|\mathbf{r} - \mathbf{r}'|) d^3r d^3r' + \frac{1}{2} \int \int \rho_s(\mathbf{r}, \mathbf{r}') \rho_{s'}(\mathbf{r}, \mathbf{r}') v_{ex}^{ss'}(|\mathbf{r} - \mathbf{r}'|) d^3r d^3r' \right], \quad (4)$$

where, the first term is the kinetic energy, second and third terms are direct and exchange contributions of the nuclear interaction; $\tau_n(\mathbf{r})$, $\rho_s(\mathbf{r})$ and $\rho_s(\mathbf{r}, \mathbf{r}')$ with $s = n, p$ are the respective kinetic energy densities, densities and density matrices which are expressed in terms of single particle wave functions as,

$$\begin{aligned} \tau(\mathbf{r}) &= \sum_{i=1}^A \nabla \phi_i^*(\mathbf{r}) \cdot \nabla \phi_i(\mathbf{r}) \\ \rho(\mathbf{r}) &= \sum_{i=1}^A \phi_i^*(\mathbf{r}) \phi_i(\mathbf{r}) \\ \rho(\mathbf{r}, \mathbf{r}') &= \sum_{i=1}^A \phi_i^*(\mathbf{r}) \phi_i(\mathbf{r}') \end{aligned} \quad (5)$$

In these expressions $\phi_i(\mathbf{r})$ are single particle wave functions, where the subscript i denotes all the quantum numbers. Instead of going into the Hartree-Fock calculation of single particle states we have adopted a theoretically transparent and numerically simplified approach where the density matrix expansion (DME) of Negele and Vautherin [41] is used for the density matrices in the exchange interaction term of the energy expression in Eq.(4). The density matrix under the DME can be expressed as,

$$\begin{aligned} \rho(\mathbf{R} + \frac{\mathbf{t}}{2}, \mathbf{R}' - \frac{\mathbf{t}}{2}) &= \frac{3j_1(k_f(\mathbf{R})\mathbf{t})}{k_f(\mathbf{R})\mathbf{t}} \rho(\mathbf{R}) \\ &+ \frac{35j_3(k_f(\mathbf{R})\mathbf{t})}{2k_f^3(\mathbf{R})} \left[\frac{1}{4} \nabla^2 \rho(\mathbf{R}) - \tau(\mathbf{R}) \right. \\ &\quad \left. + \frac{3}{5} k_f^2(\mathbf{R}) \rho(\mathbf{R}) \right] + \dots, \end{aligned} \quad (6)$$

where, j_1 and j_3 are spherical Bessel functions of order 1 and 3 respectively, $k_f(\mathbf{R})$ is the Fermi momentum corresponding to density $\rho(\mathbf{R})$ at the center-of mass \mathbf{R} of the

two interacting nucleons. Now choosing the Fermi momentum in the form [42],

$$q_f^2(\mathbf{R}) = \frac{5[\tau(\mathbf{R}) - \frac{1}{4}\nabla^2\rho(\mathbf{R})]}{3\rho(\mathbf{R})}, \quad (7)$$

reduces the DME in eq.(6) to the well known Slater approximation $\rho(\mathbf{R} + \frac{\mathbf{t}}{2}, \mathbf{R}' - \frac{\mathbf{t}}{2}) = \frac{3j_1(q_f(\mathbf{R})t)}{q_f(\mathbf{R})t}\rho(\mathbf{R})$ of the exchange term but with a modified Fermi momentum that accounts for the surface corrections up to second order in the Thomas-Fermi model. We can now express the nuclear part of the energy in eq.(4) as

$$E^{nuc} = \int H(\mathbf{R})d^3R, \quad (8)$$

where, $H(\mathbf{R})$ is the energy density given by,

$$\begin{aligned} H(\mathbf{R}) = & \frac{\hbar^2}{2M}[\tau_n(\mathbf{R}) + \tau_p(\mathbf{R})] \\ & \times \sum_{s,s'=n,p} \frac{1}{2} \left[\rho_s(\mathbf{r}) \int \rho_{s'}(\mathbf{r}') v_d^{ss'}(|\mathbf{r} - \mathbf{r}'|) d^3r' \right. \\ & \left. + \rho_s(\mathbf{r}) \rho_{s'}(\mathbf{r}') \int \frac{3j_1(q_s(\mathbf{R})t)}{q_s(\mathbf{R})t} \frac{3j_1(q_{s'}(\mathbf{R})t)}{q_{s'}(\mathbf{R})t} v_{ex}^{ss'}(t) d^3t \right] \quad (9) \end{aligned}$$

with t being the relative coordinate and q_s , $s = n, p$ is the corresponding modified Fermi momentum that can be defined from eq.(7). The calculation of energy of a nucleus now requires the knowledge of density and kinetic energy density. Wood-Saxon density distribution,

$$\rho(r) = \frac{\rho_0}{1 + \exp[(r - c)/a]} \quad (10)$$

is taken for simplicity that gives good description in the intermediate and heavy mass region. Further we make the approximation that ρ_n and ρ_p are proportional to neutron and proton numbers N and Z respectively. The kinetic energy density $\tau_s(\mathbf{R})$, $s = n, p$ is taken to be the Thomas-Fermi one along with the second order correction,

$$\tau_s(\mathbf{R}) = \frac{3}{5}k_s^2\rho(\mathbf{R}) + \frac{1}{36} \frac{[\nabla\rho_s(\mathbf{R})]^2}{\rho_s(\mathbf{R})} + \frac{1}{3}\nabla^2\rho_s(\mathbf{R}), \quad (11)$$

where, $k_{n(p)}(\mathbf{R}) = [3\pi^2\rho_{n(p)}(\mathbf{R})]^{1/3}$ is the neutron (proton) Fermi momentum at density $\rho_{n(p)}(\mathbf{R})$. The WS parameters ρ_0 , c and a are determined by minimizing the total energy, including Coulomb and center-of-correction, with respect to these parameters. The Coulomb energy of the nucleus, both direct and exchange parts, has been calculated for the WS charge distribution. In minimizing the total energy we have taken $a = 0.47$ fm and used the normalization $A = \int \rho(\mathbf{r})d^3r$ to express ρ_0 in terms of c that reduces the minimization of the total energy with respect to c only. Now, varying t_0 the minimization with respect to c is done for the experimental value of the total energy of ^{40}Ca . The parameter $t_0 = 481.86$ MeV fm³ thus obtained for the EOS having $\gamma = 1/2$ and $(\varepsilon_{ex}^l + \varepsilon_{ex}^{ul})/3$ predicts the charge radius of ^{40}Ca to be 3.49 fm as well

as the binding energies and charge radii of the closed shell nuclei over the periodic table to an satisfactory extent as given in Table-1. On varying x_0 from -1 to +1 the binding energies of $N \neq Z$ closed shell nuclei show a slow variation from a relatively smaller value to a higher value of the binding energies as compared to the results for $x_0 = 0$ given in table-1. In view of the small variation we have taken $x_0 = 0$ in rest of our calculations that makes the t_0 part of the interaction spin independent. With the value of the t_0 thus obtained for the EOS, the binding energies of the proton radioactive nuclei have been calculated using the same minimization procedure with respect to the WS parameters and it has been found that the results are reproduced within 1/2% of the experimental values for these nuclei. The WS density distributions thus obtained for these proton radioactive nuclei are used in the evaluation of the p-N interaction potentials in order to calculate the half-lives.

Table 1. Binding energies B and charge radii r_c of the closed shell nuclei. The experimental values are given besides the calculated ones inside the parenthesis.

Nucleus	B [MeV]	r_c [fm]
^{48}Ca	415.403 (415.991)	3.681 (3.484)
^{90}Zr	780.928 (783.893)	4.373 (4.272)
^{132}Sn	1091.70 (1102.86)	4.936 (- - -)
^{208}Pb	1628.246 (1636.446)	5.664 (5.505)

2.4 Nuclear part of p-N interaction potential with the YENI

The p-N nuclear interaction potential given in Eq.(1) for the YENI in Eq.(3) becomes,

$$V_N(\mathbf{r}) = V_N^{zero}(\mathbf{r}) + V_{N,dir}^{finite}(\mathbf{r}) + V_{N,ex}^{finite}(\mathbf{r}) + V_N^{rearr}(\mathbf{r}), \quad (12)$$

where V_N^{zero} contains both direct and exchange contributions from the zero range parts of the interaction, $V_{N,dir}^{finite}$ denotes the contribution from the finite range direct (exchange) part of the interaction and V_N^{rearr} is the rearrangement contribution. These various contributions are given by

$$\begin{aligned} V_N^{zero}(\mathbf{r}) = & \frac{t_0}{2}[(1 - x_0)\rho_p(\mathbf{r}) + (2 + x_0)\rho_n(\mathbf{r})] \\ & + \frac{t_3}{12}[(1 - x_3)\rho_p(\mathbf{r}) + (2 + x_3)\rho_n(\mathbf{r})]\left(\frac{\rho(\mathbf{r})}{1 + b\rho(\mathbf{r})}\right)^\gamma \\ V_{N,dir}^{finite}(\mathbf{r}) = & \frac{4\pi(W+B/2-H-M/2)}{\mu^2} \left[\frac{e^{-\mu r}}{r} \right. \\ & \left. \int_0^r r' \rho_p(\mathbf{r}') \sinh(\mu r') dr' + \frac{\sinh(\mu r)}{r} \int_r^\infty r' \rho_p(\mathbf{r}') e^{-\mu r'} dr' \right] \\ & + \frac{4\pi(W+B/2)}{\mu^2} \left[\frac{e^{-\mu r}}{r} \int_0^r r' \rho_n(\mathbf{r}') \sinh(\mu r') dr' \right. \\ & \left. + \frac{\sinh(\mu r)}{r} \int_r^\infty r' \rho_n(\mathbf{r}') e^{-\mu r'} dr' \right] \\ V_{N,ex}^{finite}(\mathbf{r}) = & \frac{2\pi(M-W/2+H/2-B)}{\mu r} \end{aligned}$$

$$\begin{aligned}
& \times \int_0^\infty r' dr' \int_{|\mathbf{r}-\mathbf{r}'|}^{|\mathbf{r}+\mathbf{r}'|} \rho_p(\mathbf{R}) \frac{3j_1[q_p(\mathbf{R})t]}{q_p(\mathbf{R})t} j_0(k(\mathbf{R})t) e^{-\mu t} dt \\
& \quad + \frac{2\pi(M+H/2)}{\mu r} \\
& \times \int_0^\infty r' dr' \int_{|\mathbf{r}-\mathbf{r}'|}^{|\mathbf{r}+\mathbf{r}'|} \rho_n(\mathbf{R}) \frac{3j_1[q_n(\mathbf{R})t]}{q_n(\mathbf{R})t} j_0(k(\mathbf{R})t) e^{-\mu t} dt \\
V_N^{rearr}(\mathbf{r}) = & \frac{t_3}{12} [(1-x_3) \frac{\rho_n^2(\mathbf{r}) + \rho_p^2(\mathbf{r})}{2} + (2+x_3) \rho_n(\mathbf{r}) \rho_p(\mathbf{r})] \\
& \times \frac{\gamma \rho^{\gamma-1}(\mathbf{r})}{[1+b\rho(\mathbf{r})]^{\gamma+1}}. \tag{13}
\end{aligned}$$

In obtaining $V_{N,ex}^{finite}$ in Eq.(13), we have approximated the density matrices $\rho_i(\mathbf{r}, \mathbf{r}')$, $i = n, p$ by their respective Slater terms,

$$\rho_i(\mathbf{r}, \mathbf{r}') \approx \frac{3j_1(q_i(\mathbf{R})t)}{q_i(\mathbf{R})t} \rho_i(\mathbf{R}) \tag{14}$$

with modified Fermi momentum $q_{n(p)}(\mathbf{R}) = [3\pi^2 \rho_{n(p)}(\mathbf{R})]^{1/3}$ that can be defined from Eq.(7). The zeroth order Bessel function $j_0(k(\mathbf{R})t)$ appearing in the expression of $V_{N,ex}^{finite}(\mathbf{R})$ is a function of the wave number $k(\mathbf{R})$ of the emitted proton that contains the potential $V_N(\mathbf{R})$ itself as can be seen from Eq.(2) and hence required to be evaluated self consistently.

The p-N nuclear part of the potential, $V_N(\mathbf{r})$, in the cases of different proton radioactive nuclei are calculated from Eqs.(12,13) for a given EOS with the WS density distributions of the nuclei obtained from the minimization procedure discussed in the last sub-section. We have considered altogether five EOSs, two cases of different p-n effective mass splittings and three cases of nuclear matter incompressibility. In case of each of the five EOSs the parameter t_0 is obtained as discussed in the last subsection and the binding energies of the nuclei are verified to be reproduced within the same accuracy in each case. The two cases of effective mass splitting in nuclear matter at normal density ρ_0 corresponding to the values of $\varepsilon_{ex}^l = (\varepsilon_{ex}^l + \varepsilon_{ex}^{ul})/6$ and $(\varepsilon_{ex}^l + \varepsilon_{ex}^{ul})/2$ are shown as a function of asymmetry $\beta = \frac{\rho_n - \rho_p}{\rho_n + \rho_p}$ in Figure-1. The results of the calculations of $V_N(\mathbf{r})$ for different radioactive nuclei for these two cases of ε_{ex}^l having a given γ value show little difference. In view of this insensitivity of the p-N interaction potential to the n-p effective mass splitting we have considered a representative value, $\varepsilon_{ex}^l = (\varepsilon_{ex}^l + \varepsilon_{ex}^{ul})/3$, in our subsequent calculations of p-N potentials for the three different cases of γ , namely, $\gamma = 1/3, 1/2$ and $2/3$, corresponding to the values of nuclear matter incompressibility 220, 240 and 253 MeV, respectively. The results of $V_N(\mathbf{r})$ for these three EOSs are shown in Figure-2 for the case of ^{113}Cs . The difference in the results in these three cases are small having the characteristic behaviour of small extension of the tail in case of lower incompressibility. We shall examine the effect of these variations in $V_N(\mathbf{r})$ on the proton half-lives.

2.5 Coulomb part of p-N interaction potential

The direct and exchange parts of the Coulomb interaction potential of a proton with a nucleus having charge distribution $\rho_p(r)$ are given by

$$V_C^{dir}(r) = 4\pi e^2 \left[\frac{1}{r} \int_0^r r'^2 \rho_p(r') dr' + \int_r^\infty r' \rho_p(r') dr' \right] \tag{15}$$

and

$$V_C^{ex}(r) = -e^2 \left(\frac{3}{\pi} \right)^{\frac{1}{3}} \rho_p^{\frac{1}{3}}(r'), \tag{16}$$

respectively. The total Coulomb potential $V_C(r) = V_C^{dir}(r) + V_C^{ex}(r)$. The Coulomb potential between the emitted proton and the daughter nucleus is calculated from Eqs.(15) and (16) using the WS proton distribution of the daughter nucleus.

3 Proton radioactivity

In the present work, the tunneling probability of the protons is calculated in the WKB framework. The WKB method has been found to be quite satisfactory for the α decay half life calculations and somewhat better than the S-matrix method [43]. The barrier penetrability P in the improved WKB [44] framework for any continuous (rounded) potential barrier is given by

$$P = 1/[1 + \exp(K)] \tag{17}$$

and the decay constant by $\lambda = \nu P S_p$ where S_p is the spectroscopic factor and the assault frequency ν is calculated from $E_v = \frac{1}{2} h \nu$, the zero point vibration energy. The half life is obtained from $T_{1/2} = \ln 2 / \lambda$. The decay half life $T_{1/2}$ of the parent nucleus (A, Z) into a proton and a daughter (A_d, Z_d) can, therefore, be given by

$$T_{1/2} = [(h \ln 2) / (2 S_p E_v)] [1 + \exp(K)] \tag{18}$$

where the action integral K within the improved WKB approximation is given by

$$K = (2/\hbar) \int_{R_a}^{R_b} [2\mu(V(r) - E_v - Q)]^{1/2} dr \tag{19}$$

with R_a and R_b being its 2^{nd} and 3^{rd} turning points determined from the equations

$$E(R_a) = Q + E_v = E(R_b) \tag{20}$$

whose solutions provide three turning points. The proton oscillates between the first and the second turning points and tunnels through the barrier at R_a and R_b . The zero point vibration energy E_v is assumed to be proportional to Q value of the spontaneous emission of protons. For the present calculations, the zero point vibration energies used here are the same as given by Eq.(5) of Ref. [45] but extended to protons and the experimental Q values [1] are used. The spectroscopic factor appearing in the denominator in Eq.(18) contribute a term $-\log S_p$ to $\log T_{1/2}$.

Table 2. Comparison between the measured and theoretically calculated half lives of proton emitters. The experimental Q values, half lives and l values are from Ref. [1]. The results of the present calculations using the YENI folded potentials are compared with the experimental values along with the results of DDM3Y [7] and GLDM [12]. The turning points $R_2=R_a$ and $R_3=R_b$ are for YENI folded potentials for the case of $\gamma=1/2$ and $\varepsilon_{ex}^l = (\varepsilon_{ex}^l + \varepsilon_{ex}^{ul})/3$. Experimental errors in Q values [1] and corresponding errors in calculated half lives are inside parentheses. Asterisk symbol in the parent nucleus denotes isomeric state.

Parent A_Z	l \hbar	Q^{ex} MeV	$R_2 = R_a$ [fm]	$R_3 = R_b$ [fm]	Measured $\log_{10}T(s)$	YENI $\log_{10}T(s)$	S_p^{expt}	S_p^{th}	GLDM $\log_{10}T(s)$	DDM3Y $\log_{10}T(s)$
^{105}Sb	2	0.491(15)	6.61	134.30	$2.049^{+0.058}_{-0.067}$	2.01(46)	0.914	0.999	1.831	1.90(45)
^{109}I	2	0.829(3)	6.69	83.29	$-3.987^{+0.020}_{-0.022}$	-4.20(4)	0.612	—	—	-4.31(5)
^{112}Cs	2	0.824(7)	6.72	88.61	$-3.301^{+0.082}_{-0.097}$	-3.10(11)	1.589	—	—	-3.21(11)
^{113}Cs	2	0.978(3)	6.78	73.45	$-4.777^{+0.018}_{-0.019}$	-5.51(4)	0.185	—	—	-5.61(4)
^{145}Tm	5	1.753(10)	6.70	56.27	$-5.409^{+0.109}_{-0.146}$	-5.25(7)	1.442	0.580	-5.656	-5.28(7)
^{147}Tm	5	1.071(3)	6.73	88.65	$0.591^{+0.125}_{-0.175}$	0.85(4)	1.816	0.581	0.572	0.83(4)
$^{147}Tm^*$	2	1.139(5)	7.25	78.97	$-3.444^{+0.046}_{-0.051}$	-3.38(6)	1.159	0.953	-3.440	-3.46(6)
^{150}Lu	5	1.283(4)	6.77	78.23	$-1.180^{+0.055}_{-0.064}$	-0.72(4)	2.884	0.497	-1.309	-0.74(4)
$^{150}Lu^*$	2	1.317(15)	7.27	71.79	$-4.523^{+0.064}_{-0.301}$	-4.37(15)	1.422	0.859	-4.755	-4.46(15)
^{151}Lu	5	1.255(3)	6.79	78.41	$-0.896^{+0.011}_{-0.012}$	-0.80(4)	1.247	0.490	-1.017	-0.82(4)
$^{151}Lu^*$	2	1.332(10)	7.32	69.63	$-4.796^{+0.026}_{-0.027}$	-4.88(10)	0.824	0.858	-4.913	-4.96(10)
^{155}Ta	5	1.791(10)	6.88	57.83	$-4.921^{+0.125}_{-0.125}$	-4.79(7)	1.352	0.422	-2.410	-4.80(7)
^{156}Ta	2	1.028(5)	7.37	94.18	$-0.620^{+0.082}_{-0.101}$	-0.39(7)	1.698	0.761	-0.642	-0.47(8)
$^{156}Ta^*$	5	1.130(8)	6.86	90.30	$0.949^{+0.100}_{-0.139}$	1.52(10)	3.724	0.493	0.991	1.50(10)
^{157}Ta	0	0.947(7)	7.48	98.95	$-0.523^{+0.075}_{-0.198}$	-0.41(12)	1.297	0.797	-0.170	-0.51(12)
^{160}Re	2	1.284(6)	7.43	77.67	$-3.046^{+0.075}_{-0.056}$	-3.01(7)	1.086	0.507	-3.111	-3.08(7)
^{161}Re	0	1.214(6)	7.55	79.33	$-3.432^{+0.045}_{-0.049}$	-3.44(7)	0.982	0.892	-3.319	-3.53(7)
$^{161}Re^*$	5	1.338(7)	6.94	77.47	$-0.488^{+0.056}_{-0.065}$	-0.73(7)	0.528	0.290	-0.677	-0.75(8)
^{164}Ir	5	1.844(9)	7.02	59.97	$-3.959^{+0.190}_{-0.139}$	-4.06(6)	0.793	0.188	-4.214	-4.08(6)
$^{165}Ir^*$	5	1.733(7)	7.03	62.35	$-3.469^{+0.082}_{-0.100}$	-3.66(5)	0.644	0.187	-3.460	-3.67(5)
^{166}Ir	2	1.168(8)	7.49	87.51	$-0.824^{+0.166}_{-0.273}$	-1.12(10)	0.506	0.415	-1.099	-1.19(10)
$^{166}Ir^*$	5	1.340(8)	7.01	80.67	$-0.076^{+0.125}_{-0.176}$	0.07(9)	1.400	0.188	-0.025	0.06(9)
^{167}Ir	0	1.086(6)	7.61	91.08	$-0.959^{+0.024}_{-0.025}$	-1.26(8)	0.500	0.912	-1.074	-1.35(8)
$^{167}Ir^*$	5	1.261(7)	7.03	83.82	$0.875^{+0.098}_{-0.127}$	0.55(8)	0.473	0.183	0.858	0.54(8)
^{171}Au	0	1.469(17)	7.67	69.09	$-4.770^{+0.185}_{-0.151}$	-5.01(16)	0.575	0.848	-4.872	-5.10(16)
$^{171}Au^*$	5	1.718(6)	7.12	64.25	$-2.654^{+0.054}_{-0.060}$	-3.18(6)	0.298	0.087	-2.613	-3.19(5)
^{177}Tl	0	1.180(20)	7.72	88.25	$-1.174^{+0.191}_{-0.349}$	-1.36(26)	0.652	0.733	-1.049	-1.44(26)
$^{177}Tl^*$	5	1.986(10)	7.20	57.43	$-3.347^{+0.095}_{-0.122}$	-4.63(6)	0.052	0.022	-3.471	-4.64(6)
^{185}Bi	0	1.624(16)	7.84	65.71	$-4.229^{+0.068}_{-0.081}$	-5.44(14)	0.062	0.011	-3.392	-5.53(14)

4 Results and conclusion

The half-lives in the cases of proton emitting nuclei away from proton drip line are calculated using the WKB barrier penetration method. The experimental Q values together with their uncertainties are considered in calculating the penetration probabilities in different proton emitting nuclei. The nuclear part of the p-N interaction potential is calculated using the semiclassical approximation up to second order for the kinetic energy densities as well as for the density matrices. The DME used for the density matrices along with the modified Fermi momenta takes care of the surface corrections up to second order. The WS density distributions of the nuclei predicted by the interaction are used to calculate the nuclear and Coulomb parts of the p-N interaction potential. The direct part of the nuclear potential is evaluated exactly whereas the exchange part is approximate up to the second order correction of the density matrix expansion. The exchange part of the nuclear potential is evaluated self consistently. The interaction potential thus obtained for the YENI effective

interaction in case of each nucleus is used to calculate the penetration probability. The half life is calculated from Eq.(15) under the consideration that the spectroscopic factor $S_p = 1$. The results of different proton emitting nuclei are given in Table 2 for the EOS corresponding to $\gamma = 1/2$ and $\varepsilon_{ex}^l = (\varepsilon_{ex}^l + \varepsilon_{ex}^{ul})/3$ along with the respective Q and l values. The results of other calculations using WKB barrier penetration are also listed in the same table for comparison together with the experimentally measured results. The agreement between the results of the present calculation and those of DDM3Y [46] are good being close to the experimental values compared to the JLM [8] model. In the JLM model the WKB penetration probabilities are calculated from the interaction potentials by folding the JLM effective interaction with the densities of the nuclei obtained from the relativistic mean field model (RMF). For the cases of ^{147}Tm , ^{150}Lu , ^{156}Ta , $^{156}Ta^*$, $^{177}Tl^*$ and ^{185}Bi . The agreement of the calculated values in the present case as well as that of DDM3Y with the experimental results do not match well. These large deviations, particularly $^{177}Tl^*$ and ^{185}Bi

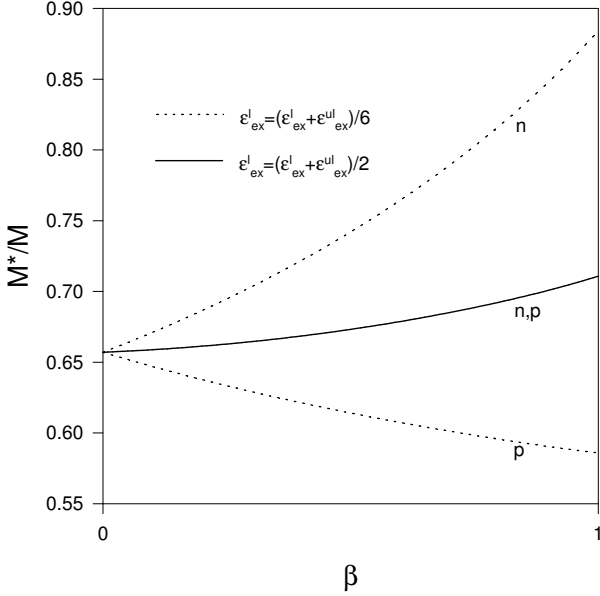


Fig. 1. Neutron and proton effective masses $[M^*(k = k_{f_{n,p}}, \rho_0, \alpha)/M]_{n,p}$ as a function of isospin asymmetry β for the two cases of splittings of exchange strength parameter into

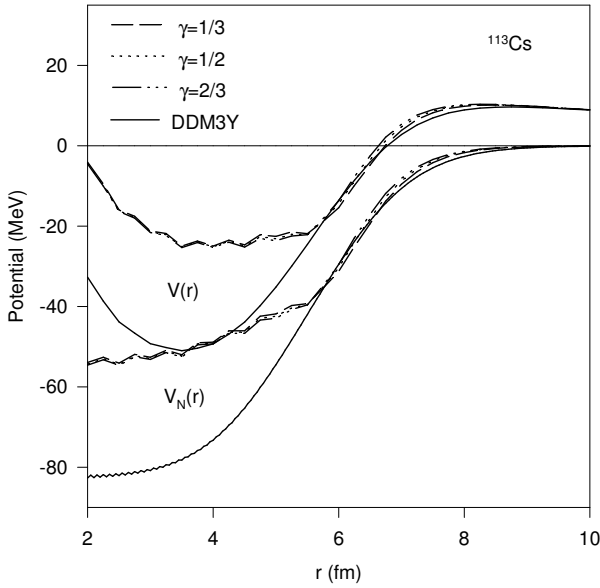


Fig. 2. The p-N potential $V(r)$ and its nuclear part $V_N(r)$ are shown as a function of distance r in case of the nucleus ^{113}Cs for DDM3Y and for three different cases of $\gamma = 1/3, 1/2$ and $2/3$. All three results corresponds to same $\epsilon_{ex}^l = (\epsilon_{ex}^l + \epsilon_{ex}^{ul})/6$. For details see the text.

could be brought down to reasonably close range of the experimental values in the GLDM model [12] calculation by including the spectroscopic factors calculated from the RMF+BCS theory. The spectroscopic factor is found to be greatly affected by the proton shell structure and in turn contains shell effect to a large extent. The uncertainty in the present calculation of half lives attributed to the spectroscopic factor can be obtained from the relation [6],

$$S_p^{expt} = \frac{T_{1/2}^{th}}{T_{1/2}^{ex}}, \text{ where } T_{1/2}^{th(ex)} \text{ is the calculated (measured)}$$

half life. The experimental spectroscopic factors S_p^{expt} obtained from this relation in the present calculation is compared with the theoretical spectroscopic factors S_p^{th} calculated using RMF+BCS model. The agreement qualitatively reproduces the general trend. It is worthwhile to mention here that the S_p^{expt} values somewhat large compared to unity such as for the cases of ^{150}Lu and $^{156}\text{Ta}^*$, can be brought down from 2.884 and 3.724 to 2.317 and 2.350, respectively, if instead of mean values extrema values of measured and theoretical half lives are used. The discrepancies may be attributed to the fact that in the present calculations the shell and deformation effects are not considered rigorously. However, in the cases where the shell effects are not strong the calculated half lives matches with the experimental ones to a reasonable extent.

The effect of n-p effective mass splitting on the decay half lives has been examined by calculating the half lives for the two cases of $\epsilon_{ex}^l = (\epsilon_{ex}^l + \epsilon_{ex}^{ul})/3$ and $(\epsilon_{ex}^l + \epsilon_{ex}^{ul})/2$. In Fig.1, the neutron and proton effective masses $[M^*(k = k_{f_{n,p}}, \rho_0, \alpha)/M]_{n,p}$ as a function of isospin asymmetry β for the two cases of splittings of exchange strength parameter into like and unlike channels. The results for half lives are almost same as expected from the results of the interaction potentials in these two cases those differ within the line width. Thus the n-p effective mass splitting in finite nuclei on the proton decay has little effect and the reason may be attributed to the fact that the asymmetry as well as the Fermi momenta involved are small. On the other hand, the effect of the variation of nuclear incompressibility show observable effect on the decay half lives. With decrease in the value of $K(\rho_0)$, the decay half lives decreases. By decreasing $K(\rho_0)$ from 240 MeV (corresponding to $\gamma = 1/2$) to 220 MeV ($\gamma = 1/3$) the results of the calculated decay half lives decrease on the average by 10%. In case of ^{113}Cs , the change in $\log_{10}T(s)$ is from -5.55 (3.12 μsec) to 5.51 (2.83 μsec) as γ decreases from 1/2 to 1/3. Similarly as $K(\rho_0)$ is increased from 240 MeV to 253 MeV by increasing γ from 1/2 to 2/3, the calculated half lives increase on the average by 7.5 % and in ^{113}Cs $\log_{10}T(s)$ is increased to -5.47 (3.39 μsec). In Fig.2, the nuclear interaction potentials $V_N(r)$ for these three EOSs of YENI have small differences in the tail region where the second turning point is located. Relatively slower rate of vanishing of the attractive nuclear potential $V_N(r)$ is observed in the tail region for the EOS corresponding to a lower value of $K(\rho_0)$ resulting in the shift of the potential barrier to higher distance. Accordingly the second turning point in this case will shift to a relatively higher distance compared to EOS corresponding to higher value

of $K(\rho_0)$. In case of ^{113}Cs in Fig.2 the position of the second turning point has decreased from 6.84 fm to 6.72 fm as $K(\rho_0)$ has increased from 220 MeV to 253 MeV. This shift in the position of the second turning point is solely determined by the nuclear part of the interaction potential as the Coulomb and the centrifugal parts are same for all these EOSs. The position of the third turning point in all the cases is solely determined from the Coulomb interaction potential that gives the same result for the different EOSs considered. Thus the width of the potential barrier in case of EOS corresponding to a lower value of incompressibility decreases in comparison to the EOS having higher incompressibility resulting in the higher penetration probability. The values of our potential and that of DDM3Y [46] in the tail region in Fig.2 are close (more so when Coulomb and centrifugal potentials are added) and hence the agreement in the results for the half lives as given in Table.2. It shows that the predictions of the proton decay half lives in different models using the WKB penetration crucially depends on the nuclear potential in the tail region that determines the position of the second turning point and hence the penetration probability.

Acknowledgement: This work is supported by the collaborative research scheme No. UGC-DAE-CSR-KC-CRS/2009/NP06/1354 of India. The work is covered under the SAP programme of School of Physics, Sambalpur University, India.

References

1. A. A. Sonzogni, Nucl. Data Sheets **95** (2002) 1.
2. C. N. Davids et al., Phys. Rev. Lett. **76** (1996) 592.
3. R. D. Page, P. J. Woods, R. A. Cunningham, T. Davinson, N. J. Davis, A. N. James, K. Livingston, P. J. Sellin and A. C. Shotton, Phys. Rev. **C 53** (1996) 660.
4. T. Enqvist, K. Eskola, A. Jokinen, M. Leino, W. H. Trzaska, J. Uusitalo, V. Ninov and P. Armbruster, Z. Phys. **A 354** (1996) 1.
5. M. Leino et al., Z. Phys. **A 355** (1996) 157.
6. S. Aberg, P. B. Semmes and W. Nazarewicz, Phys. Rev. **C 56** (1997) 1762.
7. D. N. Basu, P. Roy Chowdhury and C. Samanta, Phys. Rev. **C 72** (2005) 051601(R).
8. M. Bhattacharya and G. Gangopadhyay, Phys. Lett. **B651** (2007) 263.
9. M. Balasubramaniam and N. Arunachalam, Phys. Rev. **C 71** (2005) 014603.
10. D. S. Delion, R. J. Liotta, and R. Wyss, Phys. Rep. **424** (2006) 113.
11. F. Guzman et al., Phys. Rev. **C 59** (1999) R2339.
12. J. M. Dong, H. F. Zhang and G. Royer, Phys. Rev. **C 79** (2009) 054330.
13. Hongfei Zhang, Junqing Li, Wei Zuo, Zhongyu Ma, Baoqiu Chen and Soojae Im, Phys. Rev. **C 71** (2005) 054312.
14. G. A. Lalazissis and S. Raman, Phys. Rev. **C 58** (1998) 1467.
15. B. Behera, T. R. Routray, B. Sahoo and R. K. Satpathy, Nucl. Phys. **A 699** (2002) 770-794.
16. B. Behera, T. R. Routray, A. Pradhan, S. K. Patra and P. K. Sahu, Nucl. Phys. **A 753** (2005) 367.
17. W. Zuo, I. Bombaci and U. Lombardo, Phys. Rev. **C 60** (1999) 024605.
18. B. A. Li, Phys. Rev. **C 69** (2004) 064602.
19. Z. Y. Ma, J. Rong, B. Q. Chen, Z. Y. Zhu and H. Q. Song, Phys. Lett. **B 604** (2004) 170.
20. W. Zuo, L. G. Cao, B. A. Li, U. Lombardo and C. W. Shen, Phys. Rev. **C 72** (2005) 014005.
21. E. N. E. van Dalen, C. Fuchs and A. Faessler, Phys. Rev. Lett. **95** (2005) 022302.
22. F. Sammarruca, W. Barredo and P. Krastev, 2005 Phys. Rev. **C 71** (2005) 064306.
23. F. Hofmann, C. M. Keil and H. Lenske, Phys. Rev. **C 64** (2001) 034314.
24. S. Kubis and M. Kutschera, Phys. Lett. **B 399** (1997) 191.
25. V. Greco, M. Colonna, M. Di Toro, G. Fabbri and F. Matera, Phys. Rev. **C 64** (2001) 045203.
26. B. Liu, V. Greco, V. Baran, M. Colonna and M. Di Toro, Phys. Rev. **C 65** (2002) 045201.
27. E. Chabanat, P. Bonche, P. Haensel, J. Meyer and R. Schaeffer, Nucl. Phys. **A 627** (1997) 710; *ibid* Nucl. Phys. **A 635** (1998) 231; Nucl. Phys. **A 643** (1998) 441.
28. J. Rizzo, M. Colonna, M. Di Toro and V. Greco, Nucl. Phys. **A 732** (2004) 202.
29. T. Lesinski, K. Bennaceur, T. Duguet and J. Meyer, Phys. Rev. **C 74** (2006) 044315.
30. A. M. Lane, Nucl. Phys. **35** (1962) 676.
31. P. E. Hodgson, The Nucleon Optical Model (Singapore: World Scientific) (1994) p 613.
32. G. W. Hoffmann and W. R. Coker, Phys. Rev. Lett. **29** (1972) 227.
33. A. J. Koning and J. P. Delaroche, Nucl. Phys. **A 713** (2003) 231.
34. G. L. Thomas, B. Sinha and F. Duggan, Nucl. Phys. **A 203** (1973) 305.
35. B. Behera, T. R. Routray, A. Pradhan, S. K. Patra and P. K. Sahu, Nucl. Phys. **A 794** (2007) 132.
36. B. Behera, T. R. Routray and S. K. Tripathy, Jour. Phys. **G 36** (2009) 125105.
37. B. Behera, T. R. Routray, and R. K. Satpathy, Jour. Phys. **G 24** (1998) 2073.
38. L. W. Chen, C. M. Ko and B. A. Li, Phys. Rev. Lett. **94** (2005) 032701.
39. B. A. Li, L. W. Chen and C. M. Ko, Phys. Rep. **113** (2008) 464.
40. M. Centelles, X. R. Maza, X. Vinas and M. Warda, Phys. Rev. Lett. **102** (2009) 122502.
41. J. W. Negele and D. Vautherin, Phys. Rev. **C 5** (1972) 1472.
42. F. Hofmann and H. Lenske, Phys. Rev. **C 57** (1998) 2281.
43. S. Mahadevan, P. Prema, C. S. Shastri and Y. K. Gambhir, Phys. Rev. **C 74** (2006) 057601.
44. E. C. Kemble, Phys. Rev. **48** (1935) 549.
45. D. N. Poenaru, W. Greiner, M. Ivascu, D. Mazilu and I. H. Plonski, Z. Phys. **A 325** (1986) 435.
46. D. N. Basu, P. Roy Chowdhury and C. Samanta, Nucl. Phys. **A 811** (2008) 140.